Acta Biomaterialia 145 (2022) 272–282

Contents lists available at ScienceDirect

Acta Biomaterialia

journal homepage: www.elsevier.com/locate/actbio

Full length article

Hyphal systems and their effect on the mechanical properties of fungal sporocarps

Debora Lyn Porter*, Steven E. Naleway

The University of Utah Department of Mechanical Engineering, 1495 E 100 S Salt Lake City, Utah 84112, United States

ARTICLE INFO

Article history:
Received 29 December 2021
Revised 5 April 2022
Accepted 7 April 2022
Available online 12 April 2022

Keywords:
Fungi
Mechanical properties
Material science
Hyphae

ABSTRACT

Little is known about the mechanical and material properties of hyphae, the single constituent material of *Agaricomycetes* fungi, despite a growing interest in fungus-based materials. In the *Agaricomycetes* (the mushrooms and allies), there are three types of hyphae that make up sporocarps: generative, skeletal, and ligative. All filamentous *Agaricomycetes* can be categorized into one of three categories of hyphal systems that compose them: monomitic, dimitic, and trimitic. Monomitic systems have only generative hyphae. Dimitic systems have generative and either skeletal (most common) or ligative. Trimitic systems are composed of all three kinds of hyphae. SEM imaging, compression testing, and theoretical modeling were used to characterize the material and mechanical properties of representative monomitic, dimitic, and trimitic sporocarps. Compression testing revealed an increase in the compression modulus and compressive strength with the addition of more hyphal types (monomitic to dimitic and dimitic to trimitic). The mesostructure of the trimitic sporocarp was tested and modeled, suggesting that the difference in properties between the solid material and the microtubule mesostructure is a result of differences in structure and not material. Theoretical modeling was completed to estimate the mechanical properties of the individual types of hyphae and showed that skeletal hyphae make the largest contribution to mechanical properties of fungal sporocarps. Understanding the contributions of the different types of hyphae may help in the design and application of fungi-based or bioinspired materials.

Statement of Significance

This research studies the material and mechanical properties of fungal sporocarps and their hyphae, the single constituent material of *Agaricomycetes* fungi. Though some work has been done on fungal hyphae, this research studies hyphae in context of the three hyphal systems found in *Agaricomycetes* fungi and estimates the properties of the hyphal filaments, which has not been done previously. This characterization was performed by analyzing the structures and mechanical properties of fungal sporocarps and calculating the theoretical mechanical properties of their hyphae. This data and the resulting conclusions may lead to a better design and implementation process of fungi-based materials in various applications using the properties now known or calculated.

1. Introduction

There are estimated to be millions of species of *Fungi* in the world, many of which have yet to be discovered. These fungi are found across the world in many different biomes and environments [1,2]. To enable this success, fungal structures have a range of mechanical and physical properties to fit their varied environments [3]. In recent years, there has been a growing interest in using fungi as part of innovative, more environmentally friendly manufacturing methods for common products. Several companies have used fungi as an environmentally friendly alternative to traditional materials such as packing materials [4,5], bricks [6], and even fabrics [4,7]. Designing and creating fungal products is made possible by an understanding of fungi and their mechanical properties.

One characteristic feature of fungi is their constitutive materials. Most natural materials have multiple constitutive materials that make up their basic structures. For example, bone is a combination of two constitutive materials: collagenous fibers and hydroxyapatite crystals [8]. However, there is only one constitutive material for most species in the *Agaricomycetes,* which includes

* Corresponding author.
E-mail address: deboralyn.porter@utah.edu (D.L. Porter).

https://doi.org/10.1016/j.actbio.2022.04.011
1742-7061/

most mushroom-forming fungi: filamentous hyphae with chitinous cell walls. Hyphae are fibrous structures made up of fungal cells [9]. Hyphae can agglomerate and fuse to form mycelia, the vegetative portion of most *Agaricomycetes* [10]. Additionally, hyphae can come together and fuse to form fungal structures, including mycelial fans, rhizomorphs, and sporocarps (mushrooms). All the different fungal structures made by filamentous *Agaricomycetes* are made up of the agglomeration of this single hyphal building block [11].

Agaricomycetes fungi reproduce by spreading spores produced by sporocarps. Spores then can begin to produce hyphae as they germinate. These initial hyphae are called generative hyphae and are present in all filamentous *Agaricomycetes* fungi (Fig. 1a). These hyphae can be characterized by their septa, making divisions along the hyphal filament to prevent nuclei from moving from section to section during the growth process. These hyphae may also have some branching along the filaments [11]. As the name suggests, these generative hyphae can generate into other types of hyphae, depending on the organism [12].

During the life of some fungi, the generative hyphae can later develop into skeletal (Fig. 1b) or ligative (binding) hyphae (Fig. 1c). Both skeletal and ligative hyphae have thick walls and lack septa. Skeletal hyphae are unbranched, forming long, continuous filaments that are generally oriented along a specific direction[12]. Similar to the skeletons in vertebrates, skeletal hyphae act as a hyphal framework [12]. Ligative hyphae are unique in their highly branched structure. These complex branching structures can wind around and bind hyphae together [11,12]. The combination of these different hyphal types can create many unique properties and structures.

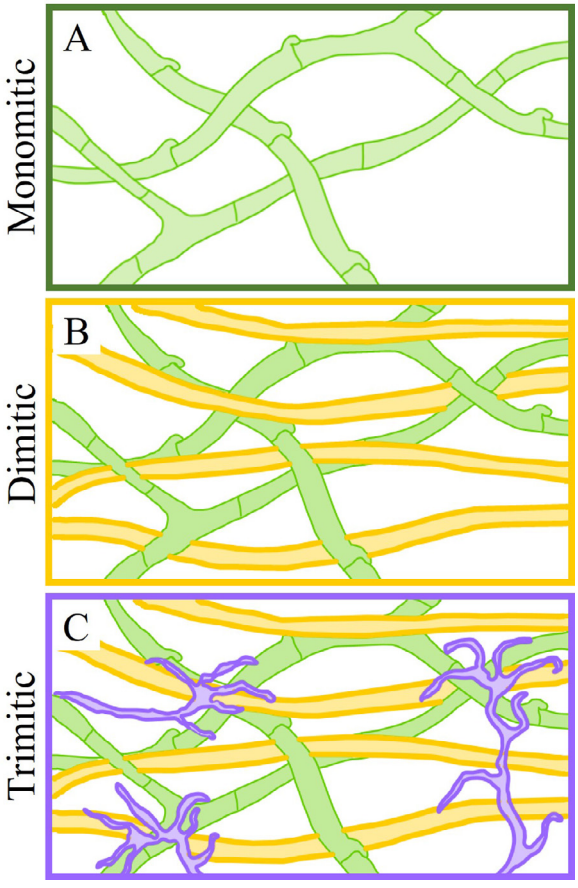

Fig. 1. Hyphal systems. A: Monomitic hyphal system with only generative hyphae (green). B: Dimitic hyphal system with generative (green) and skeletal (yellow) hyphae. C: Trimitic hyphal system with generative (green), skeletal (yellow), and ligative (purple) hyphae. (For interpretation of the references to colour in this figure legend, the reader is referred to the web version of this article.)

These three different types of hyphae can combine to make distinct hyphal systems. Based on their hyphal systems, *Agaricomycetes* fungi are categorized as one of three types: monomitic, dimitic, or trimitic fungi (Fig. 1). Monomitic fungi have only generative hyphae (Fig. 1a). Monomitic fungi include soft mushrooms, many of which are grown and sold commercially, such as white (*Agaricus bisporus*), oyster (*Pleurotus* spp.), and shiitake (*Lentinula edodes*). Dimitic fungi are generally composed of generative hyphae and skeletal hyphae (Fig. 1b), though there are some, such as the genus *Laetiporus*, which are composed of generative and ligative hyphae [11,13]. Trimitic fungi contain all three types of hyphae (Fig. 1c) and include many shelf and bracket fungi known to be tough and even woody in nature.

These different types of hyphae and fungi, and the various taxa they include, have been studied at length [11,12,14–16]. This existing literature primarily focuses on the study of hyphae and fungi from a biological or ecological perspective. Existing research on the biomechanics of fungi focuses on natural processes, such as growth, spore release, and digestion [17–23]. However, limited work has been done on the material properties, structural properties, and their connection to physical or mechanical behavior [24]. Furthermore, the contributions of the individual hyphal systems to these properties are unknown. An abundance of research has been done on other natural structures and their inherent benefits [8,25–28], laying the groundwork for the creation of bioinspired materials. Understanding the properties of fungi afforded by their constituents and structures may lead to a better understanding of their natural success in the wild, the ability to model and predict fungal behavior, and inspiration for fungus-inspired materials and designs.

In this study, we characterize material and mechanical properties of filamentous fungi and relate the macroscale properties to the micro-structures in each type of hyphal system (monomitic, dimitic, and trimitic). We used three mushrooms representative of the three hyphal systems and performed compression testing, imaging analysis and theoretical modeling to better understand this connection. This understanding of the biomechanics of fungi will advance the current knowledge of hyphal structures and their impact on properties on a larger scale. This characterization could provide a basis for better incorporation of fungi into environmentally friendly products and inform bioinspired designs.

2. Materials and methods

2.1. Sample choice and collection

Three sample types were used to analyze the different hyphal systems. White mushrooms (*Agaricus bisporus*, Fig. 2a,b) [29–31] were used as a representative monomitic sporocarp with only generative hyphae. Maitake mushrooms (*Grifola frondosa*, Fig. 2d,e) [29,32,33] were used as a representative dimitic sporocarp with generative and skeletal hyphae. Reishi mushrooms (*Ganoderma lingzhi*, Fig. 2g,h) [12,14,29,34] were used as a representative trimitic sporocarp, having generative, skeletal, and binding (ligative) hyphae. Note that, when viewed in axial cross-section, the Reishi mushrooms displayed two distinct structures. Therefore, both the top and bottom of these sporocarps were analyzed throughout this study. All three representative sporocarps are shown in Fig. 2. The sporocarps of fresh white and maitake mushrooms and a dehydrated reishi mushroom were procured from local retailers. Fresh sporocarps were dehydrated at 40 °C for 10 h in a Magic Mill® food dehydrator (Royalux Inc., Spring Valley, NY, USA). Samples taken from the dehydrated white, maitake, and reishi mushrooms

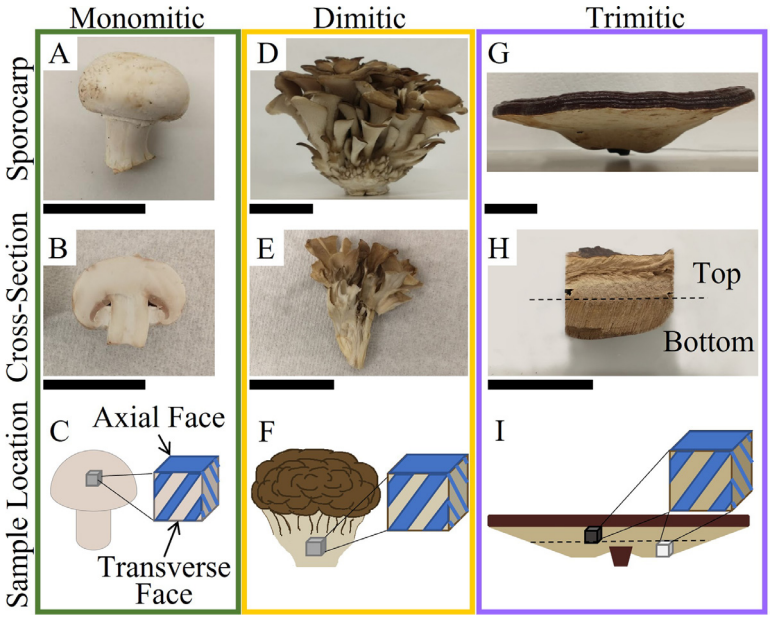

Fig. 2. Representative sporocarp samples. Images of the monomitic white mushroom (A and B), dimitic maitake mushroom (D and E), and trimitic reishi mushroom (G and H) are shown from a side view. The location from which compression and imaging samples were taken are shown (C, F, and I). The solid face of the representative sample cubes represents the axial face, and the striped faces represent the transverse faces. Note that trimitic samples are broken into top (black cube) and bottom (white cube) samples. Scale bars all represent 4 cm.

will be referred to as monomitic, dimitic, and trimitic samples, respectively.

2.2. Structural imaging and characterization

Structural analysis was completed by imaging the hyphal systems. Imaging samples were made by breaking or cutting portions off the dehydrated sporocarps for each type of hyphal system for both axial face and transverse face imaging (Fig. 2c,f,i). Imaging samples were affixed to aluminum sample holders using carbon tape and coated with ~20 nm of gold-palladium. At least three representative images were taken from each imaging sample in an FEI Quanta 600FE-ESEM scanning electron microscope (Hillsboro, OR, USA) at an accelerating voltage of 5 kV and spot size of 3 nm. Three representative images were taken of each sample type (monomitic, dimitic, trimitic-top, and trimitic-bottom) along each face (axial and transverse). Measurements of the hyphal orientation of the images was completed using ImageJ software [35]. The orientation of the hyphae was measured by converting the image to black and white, and then measuring the pores as ellipses. The angle of the major axis of the ellipses was measured, and compared to the angle of the axial direction (for images of the transverse face) or the transverse direction (for the axial face).

2.3. Mechanical testing

Compression testing was completed to characterize the mechanical properties of the different samples. Compression samples were made from the dehydrated monomitic, dimitic, and trimitic samples. Compression samples were taken from pileus (monomitic, trimitic) and stipe (dimitic) context, and hymenophore (trimitic) from the sporocarps of each specimen (Fig. 2c,f,i). Due to differentiation within the sporocarp, a longitudinal section through the pileus of the trimitic samples were split into top (pileus context) and bottom (hymenophore) sections. Twelve compression samples were made for each sample type: monomitic, dimitic, trimitic-top, and trimitic-bottom. Compression samples were roughly 6 mm tall, and with a 50 mm^2 cross-sectional area. The cross-sectional area of irregularly shaped compression samples was calculated by taking an image of the sample and using ImageJ software to calculate the area. The area of compression sample with rectangular cross sections was calculated by measuring the edges with calipers. These areas were used to calculate the stress during compression. The height of each sample was measured with calipers. The height was used to calculate the strain during testing. All measurements were made by measuring on the millimeter scale with two decimal places of precision. Six of the compression samples of each sample type were compressed axially, meaning perpendicular to the axial face. The other six samples were compressed transversely, meaning perpendicular to the transverse face. Samples were all compressed using an Instron 4303 with a 30 kN load cell. A cross-head rate of 1 mm/min was used in all tests.

After obtaining the stress-strain behavior of the sporocarp samples, material properties were calculated using MATLAB (MathWorks, Natick, MA, USA). The compression modulus (denoted E) was calculated by finding the slope of the linear portion of each of the curves. The compressive strength was calculated by finding the stress of the plateaus, which occurred after yielding. In the cases where no obvious plateau existed, the compressive strength was determined to be the point before bulk compression, indicated by the sharp increase of the slope of the curve.

2.4. Density calculation

The density of each of the sporocarp types was calculated using the volume and mass of the dehydrated compression samples prior to compression. The volume was calculated by measuring the cross-sectional area and height of each sample. The mass of each sample was then measured by weighing them on a scale. Density was calculated by dividing the mass of each sample by the respective volume. Twelve samples of each sporocarp type (monomitic, dimitic, and trimitic-top) were used in calculating the average density for each type of sample.

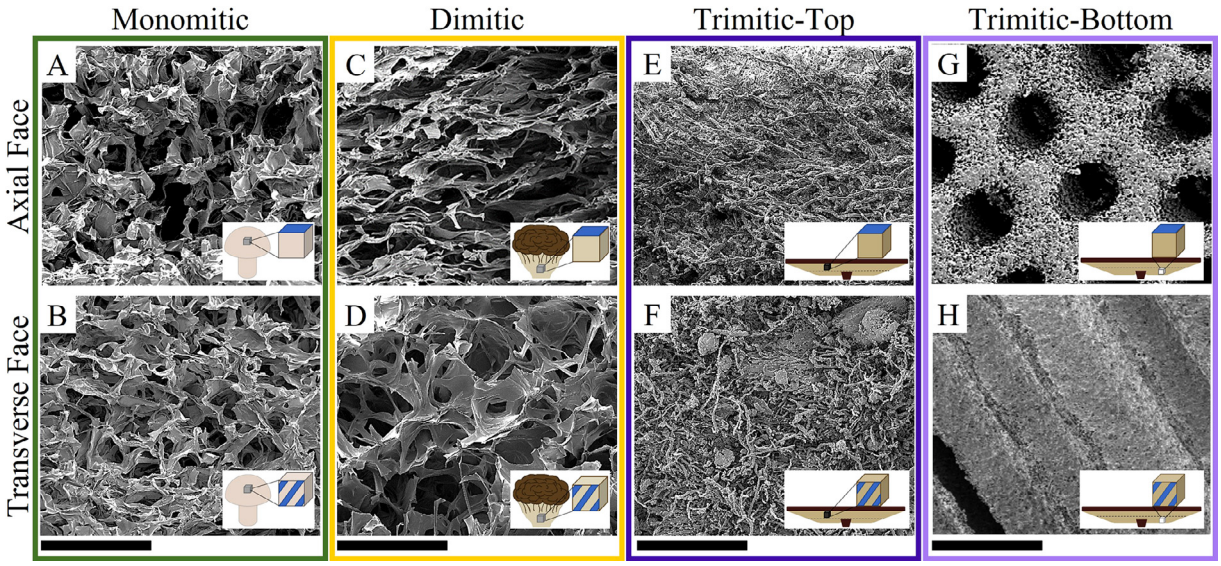

Fig. 3. Representative SEM images of the hyphal systems found in the monomitic (A, B), dimitic (C, D), trimitic-top (E, F), and trimitic-bottom (G, H) samples. Both axial faces (A, C, E, G) and transverse (B, D, F, H) faces are shown. Scale bar represents 100 μm (A, B, C, D, E, F) and 250 μm (G, H).

2.5. Statistical analysis

Statistical significance was determined by completing two-tailed, two-sample t-tests. Pairwise comparisons were completed for each type of sample. In all cases, statistical significance was determined using a confidence level of $\alpha = 0.05$.

3. Results and discussion

3.1. Structural imaging and analysis

Hyphal systems were visible in the images taken from each of the representative sporocarp samples (Fig. 3). Each of the sporocarp samples showed a porous structure, though the trimitic-top samples appear more dense (Fig. 3e,f). There was little difference between the images taken from the axial and transverse faces of the monomitic imaging samples (Fig. 3a,b). Both faces showed a loosely woven hyphal system. In contrast, the different faces of the dimitic samples showed a difference in how hyphae were oriented. The hyphae on the axial face of the dimitic samples were oriented along the transverse direction (Fig. 3c). The transverse face of the dimitic imaging samples (Fig. 3d) appeared more similar to monomitic samples, where there was no clear orientation. Similarly, the hyphae on the axial face of the trimitic-top samples were transversely oriented (Fig. 3e), whereas no clear orientation existed on the transverse face. Of interest, the trimitic-bottom samples showed a clear mesostructure of axially oriented microtubules formed by fused hyphae (Fig. 3g,h).

Microstructural directionality of the sporocarps was determined by analyzing the hyphal orientation in each of the samples (Fig. 4). There was a relatively even distribution of pore direction for both the axial and transverse faces of the monomitic samples (Fig. 4a,b). The transverse faces of the dimitic and trimitic-top samples showed a similar even distribution of hyphae angle (Fig. 4d,f). The trimitic-bottom samples were omitted due to the presence of the axially oriented microtubule mesostructure that makes up the hymenophore of the sporocarp. The monomitic, dimitic, and trimitic-top samples did not contain any mesostructures from the hymenophores of the respective sporocarps (gills for the monomitic and pores for the dimitic and trimitic). The hyphae on the axial faces of the dimitic and trimitic-top showed a preferential orientation, which aligned with the direction of transverse loading completed for mechanical testing (Fig. 4c,e).

The hyphal systems seen through SEM imaging are consistent with what has previously been studied about these different systems. Each of the sporocarps is composed of these hyphal filaments, without any additional constituent materials. Yet, these filaments remain separate, rather than fusing into a single mass. This creates porous materials that are less dense than solid material. This porosity assists in the translocation of nutrients and fluids, which is an essential role of hyphae [36,37]. The effects of the differentiated hyphae can also be seen in the dimitic and trimitic fungi. Skeletal hyphae are known to grow according to a specific orientation [12], and both sporocarps that contain skeletal hyphae show a preferential orientation in the structure made by these hyphae (Fig. 3c,e). The addition of the ligative hyphae, which bind together the generative and skeletal hyphae, contributes to the more dense structure seen in the trimitic-top images (Fig. 3e,f). The images of the trimitic-bottom samples show that these microtubule pores, used for spore dispersal are formed by hyphae [38], just as in the other portions of sporocarp samples. All of these sporocarps, with their diverse shapes and structures are created by the organized agglomeration of hyphae.

3.2. Mechanical testing

All three types of hyphal structures showed behavior typical of polymers and biopolymers under compressive loading (Fig. 5). All samples showed some quasi-linear behavior as loading began. After yielding, the stress generally plateaued, which was indicative of the compressive strength of the sample. After this plateau, stress dramatically increased as the internal structure collapsed, and the bulk material was compressed (not shown in Fig. 5). While all the samples demonstrated this general stress-strain behavior, the individual values for the modulus, strain at yielding, and compressive strength varied widely between the different types of fungi as well as the orientation of compressive loading.

3.2.1. Compression modulus

The compression modulus of the samples increased with the increasing number of hyphal types (Fig. 6, Supplementary Table 1). There was a statistically significant difference between all the calculated average values of the compression modulus for each

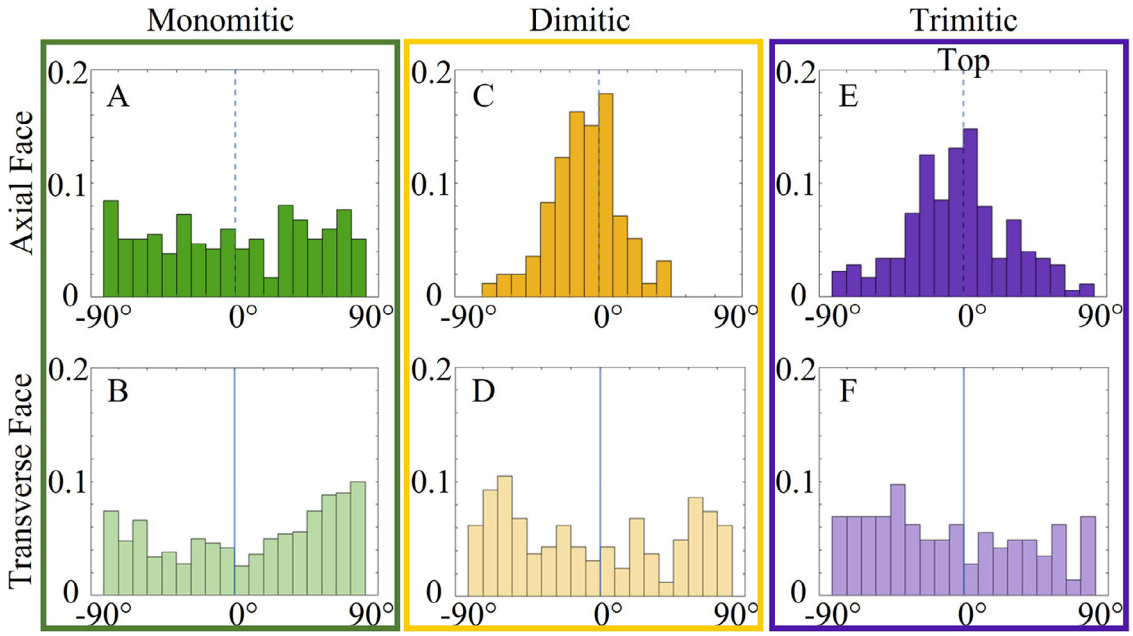

Fig. 4. Representative density histograms of the hyphal orientation of the axial and transverse faces of each of the representative sporocarps. The pore orientations of the axial faces of imaging samples are shown using dark graphs (A, C, E) and the pore orientations of the transverse faces are shown using light graphs (B, D, F). For each graph, the vertical axis represents the proportional density of pore orientation. Zero degrees represents alignment with the direction of compression. Dotted lines represent the direction of transverse compression, and solid lines represent the direction of axial compression.

sample type tested in the axial direction. The average compression modulus values of the transversely loaded sample types also had statistically significant differences, except for comparing the dimitic transverse and the trimitic-bottom transverse compression samples. For both orientations, there was a trend of increasing modulus values with more hyphal types. Monomitic samples had the smallest average modulus for both orientations (roughly 0.079 MPa in both orientations), followed by dimitic samples in the middle (0.618 MPa for axial, 2.376 MPa for transverse), and trimitic samples having the largest average modulus values. The highest compression modulus was relatively similar for both loading orientations, with trimitic-bottom samples having the highest average modulus when loaded axially (6.073 MPa) and trimitic-top samples for transverse (6.510 MPa). The maximum compression modulus value, which came from a trimitic-top sample compressed transversely, was at least 76 times as large as the average value of the monomitic samples tested in either the axial or transverse direction.

The compression modulus represents how stiff a material is under compressive loading. There is a general trend of larger compression modulus values moving from monomitic to dimitic to trimitic samples (Fig. 6). This trend suggests that the addition of hyphae increases the stiffness of the sporocarps under loading. Because skeletal hyphae act as a support structure [12], the increased modulus between the monomitic and dimitic sporocarps suggests that this structural support can provide not only a framework for

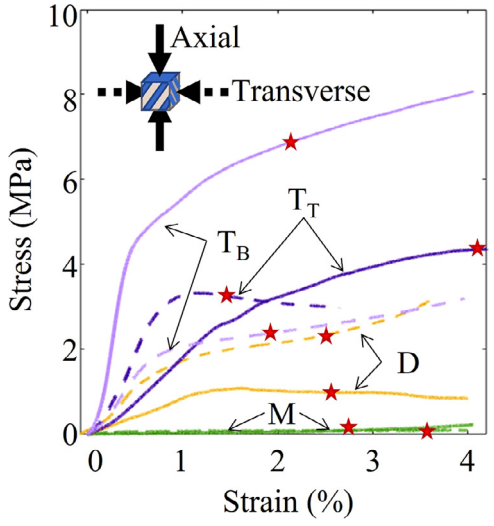

Fig. 5. Representative stress-strain behavior under compression of monomitic, dimitic, and trimitic sporocarp samples. M: monomitic; D: dimitic, T_T: trimitic-top, T_B: trimitic-bottom. Stars represent approximate location of where the compression stress was calculated.

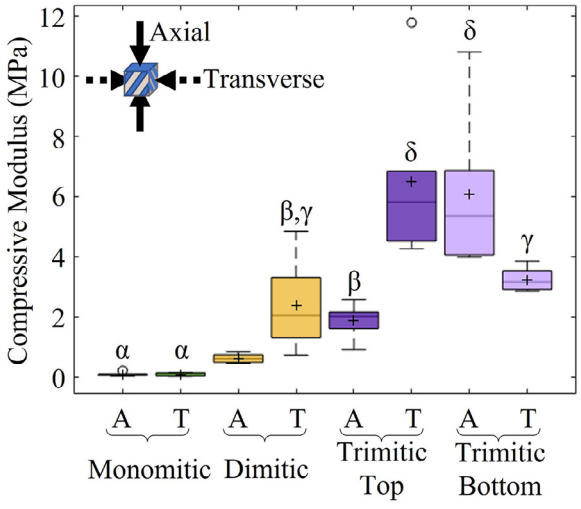

Fig. 6. Boxplots comparing the compression modulus of each of the hyphal systems and orientations (A: axial, T: transverse). Mean values are shown using a plus sign ($N = 6$). Samples with the same Greek letter above the box indicate there is no statistically significant ($p < 0.05$) difference between the two sets of data.

the shape of the structure but also enhance the stiffness of the sporocarp. The addition of ligative hyphae in the trimitic samples further increases the stiffness of the sporocarp. As the ligative hyphae bind the generative and skeletal hyphae together, the microstructure is reinforced, affecting the sporocarp properties on the macroscale. However, the degree to which the modulus is enhanced is also based on the orientation of the sporocarp during loading.

The comparison of the axial and transverse data gives insight into the effects of orientation on mechanical resistance. Isotropic properties are not dependent on directionality, whereas anisotropic properties are dependent on directionality. The modulus of the monomitic samples was isotropic, as there was no statistically significant difference in the modulus when loaded axially or transversely. Functionally, this means that when the cap of this sporocarp is loaded, it will be as stiff in one direction as another, providing no added mechanical strength based on directionality. Both the dimitic and trimitic sporocarps demonstrated anisotropic behavior with respect to the modulus, meaning there was a statistically significant difference for each of the dimitic and trimitic samples when comparing the compression modulus from axial loading to the modulus from transverse loading. The anisotropic behavior of these sporocarps indicates that there is a larger resistance to loading in the transverse direction. These sporocarps have axially oriented hymenophores, which are essential to reproduction. The monomitic, dimitic, and trimitic-top compression samples were taken from areas of the sporocarps where the respective hymenophores (the gills of the monomitic and pores of the dimitic and trimitic) were not present. As the compression data of the trimitic-bottom samples suggests, these reproductive structures are not as stiff when loaded transversely. Having a portion of the sporocarp structure away from the hymenophore that is stronger under transverse loading may help sporocarps weather predatory attacks or mechanical loading that might otherwise hamper or destroy the reproductive ability of the sporocarp. This transverse resistance is also aided with the structure framework provided by skeletal hyphae. This increased resistance could help the sporocarps in their natural environments if they are more likely to encounter attacks or other loading scenarios from one direction. These reproductive structures may also help to improve the mechanical properties of the sporocarp. The layered nature of the trimitic sporocarp, the axially oriented bottom section to the transversely oriented top section, is like other layered structures found in other natural materials. Fish scales, insect exoskeletons, and abalone all have layered structures, which affect the material stiffness and improve its mechanical resistance [25]. This is achieved by the layering of materials with different stiffnesses. Thus, the change in structure and orientation in the trimitic sporocarp likely improves the overall mechanical resistance of the sporocarp.

3.2.2. Compressive strength

Like the average compression modulus, the compressive strength of the samples increased with the addition of hyphal types (Fig. 7, Supplementary Table 1). All axial compression samples showed a statistically significant difference in their average compressive strength values. All sample types that underwent transverse loading had statistically significant differences between their average compressive strength values, except between the trimitic-top and trimitic-bottom average stress. Monomitic samples had the smallest compressive strength (approximately 0.125 MPa) in both loading orientations. Dimitic samples maintained larger average compressive strength under loading (0.801 MPa for axial, 2.063 MPa for transverse). When tested in the axial orientation, trimitic-bottom samples had the largest average compressive strength of 6.296 MPa, more than 50 times as large as that of the monomitic samples. Trimitic-top samples had the largest average strength value for the transverse orientation (4.409 MPa), more than 35 times as large as that of the monomitic samples.

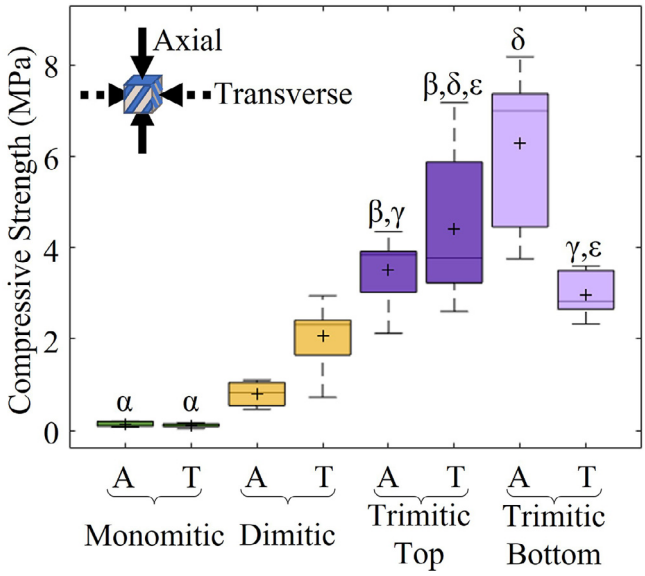

Fig. 7. Boxplots comparing the compression strength of each of the hyphal systems and orientations (A: axial, T: transverse). Mean values are shown using a plus sign ($N = 6$). Samples with the same Greek letter above the box indicate there is no statistically significant ($p < 0.05$) difference between the two sets of data.

The compressive strength represents the maximum stress the sporocarps can reach before the sample is fully densified and compressed as a bulk material. This stress can be maintained while continuing to compress the material, increasing the strain it experiences. However, this stress also occurs after yield, meaning that some damage has already been done to the structure or material by the time this stress is achieved. Maintaining this level of stress during loading allows the sporocarps to further deform and resist loading without the complete destruction of the structure, even if there is some damage done. Sporocarps with higher compressive strength have an advantage in surviving loading scenarios that might permanently damage or destroy weaker structures.

The compressive strength of the sporocarp samples showed anisotropic behavior in both the dimitic samples and the trimitic-bottom samples. Both the monomitic and trimitic-top samples showed no statistically significant difference between the compressive strength during axial and transverse loading, suggesting isotropic behavior. The compression properties (both modulus and strength) of the dimitic sporocarps were both anisotropic. The trimitic sporocarps exhibited both isotropic and anisotropic behavior, depending on the property of interest and the location of the sample on the sporocarp. The compression modulus showed anisotropic behavior for all trimitic samples. The compressive strength, on the other hand, was only anisotropic for the trimitic-bottom samples, which had a lower compressive strength that showed a statistically significant difference from the samples that were loaded transversely (Fig. 7). Other types of fungi with these tubular structures, characteristic of fungi in the *Polypore* order of fungi, have been shown to have similar mechanical resistance to loading as was seen in this study [39]. When loaded either axially or transversely, the trimitic-top samples showed no statistically significant difference in the compressive strength. Thus, the top of the representative trimitic sporocarp can maintain its maximum working stress no matter the direction of loading. This increased strength could protect the lower portion of the sporocarp, which is responsible for the dispersal of spores and propagation of the organism.

3.2.3. Effects of mesostructure

While the presence of more types of hyphae in a hyphal system can give a sporocarp added mechanical resistance to loading, the differences between the two types of trimitic samples indicate that the mechanical properties are also dependent on the mesostructures created by the sporocarps. The top of the representative trimitic sporocarp was essentially composed of bulk material. The bottom of the sample, on the other hand, has micro-tubules (see Fig. 3g,h). These tubule structures increase the fertile surface area and facilitate spore dispersal [38], and they also affect the sporocarp's mechanical properties, as seen in Sections 3.2.1 and 3.2.2. This tubular structure is commonly found in other natural materials, such as ram horn, crab exoskeleton, horse hooves, and elsewhere, and is known to increase the mechanical properties of the material when loaded parallel to the tubules by effectively employing this structure that allows for a higher modulus and strength with less bulk material [25].

We can calculate theoretical values for the compression modulus and compressive strength for these types of structures to compare to the actual measured quantities. As shown in Sections 3.2.1 and 3.2.2, the top and bottom of the representative trimitic sporocarp have different structures with different properties. It is possible that the difference in properties could be a result of a difference in materials. By comparing the actual values of the compression modulus and compressive strength of the trimitic sporocarps to expected values calculated by known models, it may be determined whether the difference in properties is purely due to structural difference of the mesostructures or if there may be some difference in the material. The compression modulus of this type of structure, compressed in the axial direction (i.e., parallel to the microtubules), can be modeled using the following equation, adapted from [25]:

$$\frac{E}{E_d} = \left(1 - V_p^2\right), \tag{1}$$

where E is the modulus of the porous material, E_d is the modulus of the dense material, and V_p is the volume fraction of the pores. Eq. (1) can be rearranged to solve for the porous material modulus (Eq. (2)) and the dense material modulus (Eq. (3)):

$$E_d = \frac{E}{1 - V_p^2}, \tag{2}$$

$$E = E_d\left(1 - V_p^2\right). \tag{3}$$

Using Eqs. (2) and (3), the trimitic-top and trimitic-bottom samples can be compared. The average trimitic-top transverse compression modulus can be used as the dense material, and the average trimitic-bottom axial compression modulus can be used as the porous. The volume fraction of the pores is $V_p = 0.3$, which was estimated through the analysis of SEM images of the bottom surface of the trimitic sporocarp (using ImageJ). Using Eqs. (2) and (3), the theoretical values for the moduli of both the dense material (E_d) and the porous material (E) are calculated. A theoretical compression modulus for the dense material was calculated using Eq. (2) and compared to the actual values from the microtubule section (trimitic-bottom axial). Then a theoretical compression modulus of the microtubule structure was calculated using Eq. (3) and compared to the modulus of the dense material (trimitic-top transverse). In both cases, calculated and actual values of the moduli were relatively similar, with a percent error of about 2.5% when calculating either the modulus of the dense material or the porous material (see Table 1).

The compressive strength, σ_c, of microtubular structures when compressed parallel to the length of the microtubules can be expressed as

$$\sigma_c = \frac{E_d\left(1 - V_p^{1/3}\right)\varepsilon_{pf}}{\nu_d}, \tag{4}$$

where E_d is the compression modulus of the dense material, V_p is the volume fraction of pores, ε_{pf} is the strain at failure of the porous microtubular structure, and ν_d is Poisson's ratio of the dense material (adapted from [25]). Because chitin is the primary component of cell walls in the fungi examined, the Poisson's ratio of the dense material can be estimated using the Poisson's ratio of chitin ($\nu_d = 0.25$) [40]. The volume fraction of pores used to calculate the compressive strength is the same as was used to calculate the structure's moduli ($V_p = 0.3$). The average strain at failure of the trimitic-bottom axial samples was used to determine the failure of the microtubular structure ($\varepsilon_{pf} = 0.73$) and the average trimitic-top transverse compression modulus was used to determine the modulus of the matrix ($E_d = 6.5096$ MPa). The percent error between the actual and the calculated compressive strength was only 0.19%, indicating that the calculated and observed values were almost identical (Table 1).

When loaded axially, the trimitic-bottom samples achieved nearly three times the compression modulus and twice the compressive strength when compared to the axially loaded trimitic-top samples. The trimitic-top samples achieved a similar average modulus to the axially loaded trimitic-bottom samples when loaded transversely. Layered structures increase the mechanical resistance of an overall structure and are found in many natural materials, such as arapaima scales and abalone [25]. However, the arapaima scales and abalone layers are composed of different materials or constituent concentrations [41,42]. The equations used to calculate the moduli and compressive strength assume that the dense and porous materials are the same. Thus, the small percent error when modeling the compression modulus and compressive strength (Table 1) suggests that the top and bottom layer of the representative trimitic sporocarp are the same materials. This is consistent with what is known about fungi and the fact that they are known to create their different structures using a single constituent [11]. The different mesostructures of the top and bottom layer of the trimitic sporocarp, made by the same constituent material and organized into distinct structures, provide properties that would not be possible with only solid material. This increased mechanical resistance afforded by the combination of layer orientations gives the representative trimitic sporocarps an added survival advantage by ensuring a damage-resistant structure, all with its single microstructural constituent material: hyphae.

3.2.4. Effects of hydration

The growing interest in fungus-based materials makes understanding fungal properties a vital aim. Fungi have been used to make alternative packaging materials [4,5], fabrics [4,7], and even bricks [6]. These applications are likely to be the first of many fungi-based environmentally friendly approaches to manufacturing materials. Each of these uses fungi in a dry, dehydrated state. Fungal sporocarps are known to be hydrophilic. Across different species, the moisture content of different sporocarps can range from roughly 17 to 89% depending on the species, age, and soil in which the sporocarp grew [43]. As such dehydrated sporocarps may not offer a good model of wildtype sporocarps. Understanding the effects that hydration can have on fungi is important, but knowing the dehydrated properties allows for a foundation of knowledge for how fungi may be grown and used in innovative applications such as leather or packing materials [5,9]. As such, each of the sporocarp types was also tested in a hydrated state and the mechanical data from these test are included in the Supplementary Materials. This data showed that hydration can drastically affect the mechanical resistance of sporocarps, with both the modu-

Table 1
Calculated values and percent error for the compression modulus of the dense material, compression modulus of the microtubular structure, and compressive strength of the microtubular structure from the trimitic samples. Actual values were from the trimitic-top transverse samples (E_d), the trimitic-bottom axial samples (E, σ_c).

Variable of Interest	Equation	Actual Value [MPa]	Calculated Value [MPa]	Percent Error [%]
E_d	(2)	6.5096	6.6737	2.46
E	(3)	6.0731	5.9237	2.52
σ_c	(4)	6.2955	6.2834	0.19

Table 2
Average density of monomitic, dimitic, and trimitic-top samples.

Sporocarp Type	Number of samples	Average Density [g cm^{-3}]
Monomitic	12	0.107
Dimitic	12	0.229
Trimitic-Top	12	0.341

lus and the strength of the samples at least an order of magnitude smaller than the dehydrated samples.

3.3. Theoretical modeling of hyphal properties

Using known models of cellular solids, the relative contributions of the generative, skeletal, and ligative hyphae to the macroscopic mechanical properties can be estimated. For the dimitic and trimitic-top samples, there is reinforcement in the transverse direction due to the orientation of the skeletal hyphae. By using the compression data (Figs. 6, 7, Supplementary Table 1) and average density (Table 2) for each type of sporocarp, the theoretical properties of each type of hyphae can be calculated. For consistency in calculating theoretical properties across sporocarp type, the compression and density values of the transversely compressed sporocarp samples were used. As seen in Fig. 3, the sporocarp samples are porous, cellular solids, with the hyphae acting as the solid edges of the cells. The modulus of the solid portion of the cells can be estimated using (adapted from [44])

$$E_s = E_p\left(\frac{\rho_s}{\rho_p}\right)^2, \tag{5}$$

where E_s is the compression modulus of the solid material, E_p is the modulus of the porous material, ρ_s is the density of the solid material, and ρ_p is the density of the porous material. Because the main constituent material of fungal cells is chitin [45], the density of the solid material was estimated using the density of chitin (ρ_s = 1.425 g/cm^3) [46]. The porous modulus E_p was the modulus calculated using compression testing (see Fig. 6) for the respective sporocarp compression samples. The density of the porous material ρ_p was the average density for each type of sample (Table 2).

Like the modulus, the compressive strength of the solid portion of the sporocarp can be modeled as (adapted from [44])

$$\sigma_s = \frac{\sigma_p}{0.3}\left(\frac{\rho_s}{\rho_p}\right)^{\frac{3}{2}}, \tag{6}$$

where σ_s is the compressive strength of the solid material, σ_p is the compressive strength of the porous material, ρ_s is the density of the solid material, and ρ_p is the density of the porous material. Using the density of chitin (ρ_s = 1.425 g/cm^3), the calculated density of compression samples, and the compressive strength of each sample (see Fig. 7), total compressive strength of the solid hyphae material can be calculated for each sample.

Because the solid material of each sporocarp is hyphae, the individual mechanical properties from Eqs. (5) and (6) can be calculated for each type of hypha. Doing so assumes that the contributions of each of the hyphal types to the overall mechanical properties of the sporocarps are additive. The properties of the generative hyphae can be found by applying Eqs. (5) and (6) to the monomitic samples. Because dimitic samples are a combination of generative and skeletal hyphae, the theoretical properties of skeletal hyphae can be calculated by subtracting the properties of the generative hyphae from the theoretical values of the dimitic samples. In a similar manner the theoretical values of the mechanical contributions of ligative hyphae can be found by looking at the theoretical values of the trimitic hyphae and subtracting the properties of both the skeletal and generative hyphae. Using this process further allows for the calculation of the overall contribution of each of these types of hyphae in a trimitic sporocarp sample (Table 3).

Generative hyphae had both the smallest theoretical modulus and compressive strength of the three types of hyphae, whereas skeletal hyphae had the greatest modulus and strength. In trimitic fungi, where all three types of hyphae are present, the addition of both ligative and skeletal hyphae contribute to a greater modulus and strength than is possible in the dimitic or monomitic fungi. The skeletal hyphae, which align and reinforce the sporocarp in a given direction [12], provide the greatest contribution to the strength and modulus of the trimitic hyphal system. The skeletal hyphae have a modulus that is more than three times as large as that of the generative hyphae and a yield strength nearly five times as large (Table 3). While the skeletal hyphae have the single largest contribution to the mechanical properties of the sporocarps, the ligative hyphae potentially made the difference in the greater strength and stiffness achieved by the trimitic sporocarp. The ligative hyphae bind together the generative and skeletal hyphae together [11,12]. This binding likely allows for an increased stiffness and strength as the material is stretched or compressed, increasing the modulus of the hyphal system. While the dimitic sporocarp compression samples had a marked increase in strength and stiffness compared to the monomitic hyphae, the addition of ligative hyphae in the trimitic compression samples was roughly double of the dimitic samples compressed in the same direction.

The modulus values calculated (Table 3), are lower than the cell wall moduli of other fungal hyphae, as measured in previous literature. Zhao et al. [47] reported the cell wall of wildtype hyphae of *Aspergillus nidulans* to have a dolulust of approximately 110 MPa. Stocks et al. [48] estimated the cell wall of *Saccharopolyspora erythraea* hyphae to have a modulus of roughly 140 MPa. While neither of these species are in the *Agaricomycetes* class of fungi, as was used in the current study when selecting representative sporocarps, this range gives an idea of the properties of the outer wall of the hyphal filaments. The lower modulus values calculated (Table 3) would reflect the differences within the different types of hyphae of each system. Skeletal and ligative hyphae are known to have a thicker cell wall than generative hyphae and different structures that would affect the properties of the overall hyphal filaments [11]. These differences between the different types of fungi and how they affect the properties of the hyphal filaments offer an interesting avenue of research in how structure of the hyphae affect its mechanical properties.

Table 3
Theoretical mechanical properties of different hyphal types and the proportion of their contribution in trimitic fungi, where all are present. Note that the modulus refers to the compression modulus of the hyphae, and the strength refers to the compressive strength of the hyphae.

	Property Contribution			
	Modulus [MPa]	Contribution to Modulus [%]	Strength [MPa]	Contribution to Yield [%]
Generative Hyphae	14	12	18	14
Skeletal Hyphae	78	69	89	71
Ligative Hyphae	21	19	18	15

Properties of natural materials come from a combination of constituent materials and structure. Many natural materials have few constituent materials [49]. Nevertheless, the structures created by natural materials allow for unexpected properties. For example, bone uses a combination of collagen and hydroxyapatite as its constituent materials. However, the measured mechanical properties are greater than would be expected by using the rule of mixtures [49]. This increase in properties is due to the structures created by the constituents at different length scales, such as rotating layers [25,49]. *Agaricomycetes* fungi have many different structures and properties, yet only have their single constituent: hyphae. The differentiation of hyphae allows for *Agaricomycetes* fungi to achieve greater resistance to mechanical loading without the addition of more constituents.

The range of properties made possible by the different hyphal systems facilitates the success of fungi in a wide range of environments. Many soft sporocarps, such as the representative monomitic and dimitic sporocarps, have a higher water content and a shorter lifespan than trimitic sporocarps [43,50]. This increase in water content of these sporocarps may allow the sporocarps to develop rapidly and continuously release spores [50]. These softer species must balance the need for more pliable material properties to assist in spore dispersal and growth with mechanical resistance in imperfect conditions. In contrast, tougher sporocarps, such as the representative trimitic sporocarp, must maintain their mechanical resistance to help ensure their longevity and chance for reproduction without sacrificing properties or structures necessary for biological processes.

Fungal sporocarps maintain strength while remaining pliable. By normalizing the compressive strength and compression modulus using the density of the respective sporocarp densities, the properties of the representative sporocarp samples can be compared to other natural materials (Fig. 8). Monomitic sporocarps have a specific modulus that is more than an order of magnitude smaller than materials such as leather or cork but have a similar specific strength. Trimitic sporocarp samples, which were shown to be the strongest and stiffest of the fungal sporocarps tested, achieve a specific strength similar to or greater than cancellous bone or wood despite having a specific modulus that is more than an order of magnitude smaller.

The theoretical strength and modulus values of the three types of hyphae can also be normalized, assuming the hyphae have a density of 1.425 g/cm^3, as was used in theoretical calculations (Fig. 8) [46]. Both the specific strength and modulus of the generative hyphae are nearly an order of magnitude larger than what was achieved by the structure of the monomitic sporocarp. The specific strength and modulus of the ligative hyphae were larger than the trimitic-top sporocarp samples, but similar to the trimitic-bottom sporocarp samples. The specific strength and modulus of the skeletal hyphae was greater than any of the sporocarp samples and achieved a specific strength greater than that of wood (Fig. 8). Interestingly, though each of the theoretical specific modulus values of the hyphae are greater than the sporocarp samples without any mesostructures (monomitic, dimitic, and trimitic-top), the way

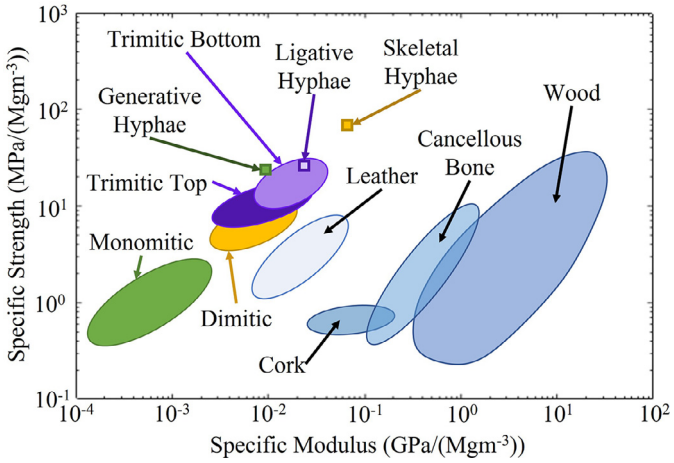

Fig. 8. Ashby plot showing the specific modulus versus the specific strength of several natural materials, including representative sporocarps and the theoretical values of generative, skeletal and ligative hyphae. Values for other natural materials are adapted from [45].

that these filaments form a porous network allows for a more flexible structure.

An advantage of hyphae being the single constituent of fungal structures is the ability to heal without the combination of any other materials. Hyphae are able to seal off after initial damage. Following initial damage, hyphae are then able to begin regrowth [51]. Wounds in fungi can heal as hyphae recognize genetically similar hyphae. These hyphae are then able to fuse together and repair damage [52,53]. This ability to regrow and fuse may give fungal sporocarps an added advantage over other natural materials which are not able to heal as effectively, such as trees. Unlike a tree that has specific nutrient transport sections [54], the sporocarps can sustain some damage due to yielding and maintain essential functions so long as they do not catastrophically fail, thus making different fungal structures damage resistant [24,55].

The results of this study are limited to the representative sporocarps tested. While these sporocarps are expected to represent the properties of other monomitic, dimitic, and trimitic hyphal systems, future work could expand this to sporocarps of other species. By selecting phylogenetic pairs with similar representative sporocarps, it could be determined whether the properties presented are consistent for the separate hyphal systems or if the properties are dependent on a species-specific trait. However, this greater understanding of hyphal systems and the mechanical properties of individual hyphal systems may allow for the creation of more fungal-based products or bioinspired materials.

In designing and manufacturing materials, the properties required for the application must be met by the material chosen. There is an interest in using fungi to manufacture goods such as faux leather or packing material. This environmentally friendly approach to manufacturing materials may continue and further ex-

pand as the material and mechanical properties of fungi are tested and described. While many of the companies that make these fungi-based materials do not disclose their proprietary process in making their products [4,7,9], common genera of fungi used include *Ganoderma* and *Pleurotis*, which are trimitic and monomitic systems, respectively [9]. Knowing the properties of these hyphal systems aids in creating and using accurate models to describe the behavior that could be used to design and of fungi-based materials in a more cost-effective manner by limiting the effort and time to grow or make the material before gaining an idea of what kind of properties are to be expected.

4. Conclusions

This study employed imaging, mechanical testing, and theoretical modeling to characterize not only the mechanical properties of fungal sporocarps, but also the contribution of individual types of hyphae. Using these methods and the analysis of the distinct results led to the following conclusions:

- The addition of hyphal types in the three representative *Agaricomycetes* sporocarps resulted in enhanced mechanical properties of the sporocarps at the macroscale. Both the compression modulus and the compressive strength increase going from the representative monomitic to dimitic to trimitic hyphal systems. This increase in mechanical resistance likely suits the specific environments of each type of sporocarp to promote survival long enough to reproduce.
- Hydration affects the mechanical properties of sporocarps. Though moisture content differs between taxa, fluctuations in the environment cause changes that may create a less hospitable environment for spore dispersal and germination. The heightened mechanical resistance of dehydrated sporocarps, which would be experienced in drier times during the year, may allow for increased survival time in which to reproduce.
- Hyphae, the single main constituent of filamentous *Agaricomycetes* sporocarps, form many different structures that can perform different functions. These structures can include mesostructures necessary for spore dispersal that also provide additional strength to the structure, as in the case of the representative trimitic fungi. Modeling indicates that these mesostructures are formed by the same material as the rest of the sporocarp, and that the increased mechanical properties are not the result of differences in material makeup.
- The theoretical compressive strength and compression modulus of the generative, skeletal, and ligative hyphae can be calculated using known models for cellular solids. This modeling of individual properties demonstrates that the skeletal hyphae make the biggest difference in the compressive stress of fungal sporocarps. Furthermore, this ability to model and predict mechanical properties may allow for the better design of fungal-based or fungal-inspired materials.

Declaration of Competing Interest

The authors declare that they have no known competing financial interests or personal relationships that could have appeared to influence the work reported in this paper.

Acknowledgements

The authors would like to acknowledge and thank Bryn T. M. Dentinger for his help and expertise throughout the course of this research.

Supplementary materials

Supplementary material associated with this article can be found, in the online version, at doi:10.1016/j.actbio.2022.04.011.

References

[1] M. Cheek, E.N. Lughadha, P. Kirk, H. Lindon, J. Carretero, B. Looney, B. Douglas, D. Haelewaters, E. Gaya, T. Llewellyn, A.M. Ainsworth, Y. Gafforov, K. Hyde, P. Crous, M. Hughes, B.E. Walker, R.C. Forzza, K.M. Wong, T. Niskanen, New scientific discoveries: plants and fungi, Plants People Planet 2 (2020) 371–388, doi:10.1002/ppp3.10148.
[2] D.L. Hawksworth, R. Lücking, Fungal Diversity Revisited: 2.2 to 3.8 Million Species, Microbiol. Spectr. 5 (2017), doi:10.1128/microbiolspec.FUNK-0052-2016.
[3] L. Boddy, Chapter 11 - Fungi, Ecosystems, and Global Change, in: S.C. Watkinson, L. Boddy, N.P. Money (Eds.), Fungi Third Ed, Academic Press, Boston, 2016, pp. 361–400, doi:10.1016/B978-0-12-382034-1.00011-6.
[4] Ecovative Design, Ecovative Des. (n.d.). https://ecovativedesign.com (accessed August 19, 2021).
[5] Sustainable Packaging | Polystyrene Alternatives, Mushroom Mater. (n.d.). https://www.mushroommaterial.com (accessed August 19, 2021).
[6] Building with Mushroom Bricks, (n.d.). https://dornob.com/fast-fungi-bricks-mushroom-blocks-better-than-concrete/ (accessed August 19, 2021).
[7] MycoWorks, MycoWorks. (n.d.). https://www.mycoworks.com/(accessed August 19, 2021).
[8] W. Huang, D. Restrepo, J.-Y. Jung, F.Y. Su, Z. Liu, R.O. Ritchie, J. McKittrick, P. Zavattieri, D. Kisailus, Multiscale Toughening Mechanisms in Biological Materials and Bioinspired Designs, Adv. Mater. 31 (2019) 1901561, doi:10.1002/adma.201901561.
[9] M.R. Islam, G. Tudryn, R. Bucinell, L. Schadler, R.C. Picu, Morphology and mechanics of fungal mycelium, Sci. Rep. 7 (2017) 13070, doi:10.1038/s41598-017-13295-2.
[10] F.V.W. Appels, H.A.B. WöstenÓ. Zaragoza, A. Casadevall (Eds.), Mycelium Materials, Encycl. Mycol. (2021) 710–718, doi:10.1016/B978-0-12-809633-8.21131-X.
[11] P. Kirk, P. Cannon, D. Minter, J. Stalpers, Dictionary of the Fungi, 10th ed., CABI Publishing, Wallingford, 2008.
[12] D.N. Pegler, Hyphal analysis of basidiomata, Mycol. Res. 100 (1996) 129–142, doi:10.1016/S0953-7562(96)80111-0.
[13] H.H. Burdsall, M.T. Banik, THE GENUS LAETIPORUS IN NORTH AMERICA, Harv. Pap. Bot. 6 (2001) 43–55.
[14] F. Hennicke, Z. Cheikh-Ali, T. Liebisch, J.G. Maciá-Vicente, H.B. Bode, M. Piepenbring, Distinguishing commercially grown Ganoderma lucidum from Ganoderma lingzhi from Europe and East Asia on the basis of morphology, molecular phylogeny, and triterpenic acid profiles, Phytochemistry 127 (2016) 29–37, doi:10.1016/j.phytochem.2016.03.012.
[15] L.-S. Lai, D.-H. Yang, Rheological properties of the hot-water extracted polysaccharides in Ling-Zhi (Ganoderma lucidum), Food Hydrocoll 21 (2007) 739–746, doi:10.1016/j.foodhyd.2006.09.009.
[16] R.A. Maas Geesteranus, Hyphal structures in Hydnums, Persoonia - Mol. Phylogeny Evol. Fungi. 2 (1962) 377–405.
[17] Y.C. Fung, Biomechanics: mechanical properties of living tissues, New York :, 1981. http://hdl.handle.net/2027/mdp.39015058309918.
[18] N.P. Money, The fungal dining habit: a biomechanical perspective, Mycologist 18 (2004) 71–76, doi:10.1017/S0269915x04002034.
[19] L. Yafetto, D.J. Davis, N.P. Money, Biomechanics of invasive growth by Armillaria rhizomorphs, Fungal Genet. Biol. 46 (2009) 688–694, doi:10.1016/j.fgb.2009.04.005.
[20] N.P. Money, Insights on the mechanics of hyphal growth, Fungal Biol. Rev. 22 (2008) 71–76, doi:10.1016/j.fbr.2008.05.002.
[21] R.R. Lew, Biomechanics of Hyphal Growth, Biomechanics of Hyphal Growth, in: D. Hoffmeister, M. Gressler (Eds.), 2019 Biol. Fungal Cell 83–94, doi:10.1007/978-3-030-05448-9_5.
[22] N.P. Money, Biomechanics of Invasive Hyphal Growth, Biomechanics of Invasive Hyphal Growth, in: R.J. Howard, N.A.R. Gow (Eds.), 2001 Biol. Fungal Cell 3–17, doi:10.1007/978-3-662-06101-5_1.
[23] N.P. Money, M.W.F. Fischer, Biomechanics of Spore Release in Phytopathogens, Biomechanics of Spore Release in Phytopathogens, in: H.B. Deising (Ed.), 2009 Plant Relatsh. 115–133, doi:10.1007/978-3-540-87407-2_6.
[24] D.L. Porter, A.J. Bradshaw, R.H. Nielsen, P. Newell, B.T.M. Dentinger, S.E. Naleway, The melanized layer of Armillaria ostoyae rhizomorphs: its protective role and functions, J. Mech. Behav. Biomed. Mater. 125 (2022) 104934, doi:10.1016/j.jmbbm.2021.104934.
[25] S.E. Naleway, M.M. Porter, J. McKittrick, M.A. Meyers, Structural Design Elements in Biological Materials: application to Bioinspiration, Adv. Mater. 27 (2015) 5455–5476, doi:10.1002/adma.201502403.
[26] M.A. Meyers, J. McKittrick, P.-Y. Chen, Structural Biological Materials: critical Mechanics-Materials Connections, Science 339 (2013) 773–779, doi:10.1126/science.1220854.
[27] M.A. Meyers, P.-Y. Chen, A.Y.-M. Lin, Y. Seki, Biological materials: structure and mechanical properties, Prog. Mater. Sci. 53 (2008) 1–206, doi:10.1016/j.pmatsci.2007.05.002.

[28] P.-Y. Chen, A.Y.-M. Lin, J. McKittrick, M.A. Meyers, Structure and mechanical properties of crab exoskeletons, Acta Biomater 4 (2008) 587–596, doi:10.1016/j.actbio.2007.12.010.
[29] Index Fungorum - Search Page, (n.d.). http://www.indexfungorum.org/Names/Names.asp (accessed August 13, 2021).
[30] R.L. Berendsen, S.I.C. Kalkhove, L.G. Lugones, H.A.B. Wösten, P.A.H.M. Bakker, Germination of Lecanicillium fungicola in the mycosphere of Agaricus bisporus, Environ. Microbiol. Rep. 4 (2012) 227–233, doi:10.1111/j.1758-2229.2011.00325.x.
[31] A.M. Vos, R.-J. Bleichrodt, K.C. Herman, R.A. Ohm, K. Scholtmeijer, H. Schmitt, L.G. Lugones, H.A.B. Wösten, Cycling in degradation of organic polymers and uptake of nutrients by a litter-degrading fungus, Environ. Microbiol. 23 (2021) 224–238, doi:10.1111/1462-2920.15297.
[32] O. Miettinen, E. Larsson, E. Sjökvist, K.-H. Larsson, Comprehensive taxon sampling reveals unaccounted diversity and morphological plasticity in a group of dimitic polypores (Polyporales, Basidiomycota), Cladistics 28 (2012) 251–270, doi:10.1111/j.1096-0031.2011.00380.x.
[33] M.L. Gargano, G.I. Zervakis, O.S. Isikhuemhen, G. Venturella, R. Calvo, A. Giammanco, T. Fasciana, V. Ferraro, Ecology, Phylogeny, and Potential Nutritional and Medicinal Value of a Rare White "Maitake" Collected in a Mediterranean Forest, Diversity (Basel). 12 (2020), doi:10.3390/d12060230.
[34] X.-C. Wang, R.-J. Xi, Y. Li, D.-M. Wang, Y.-J. Yao, The Species Identity of the Widely Cultivated Ganoderma, 'G. lucidum' (Ling-zhi), in China, PLoS ONE 7 (2012) e40857, doi:10.1371/journal.pone.0040857.
[35] Image J., (n.d.). https://imagej.nih.gov/ij/ (accessed February 9, 2022).
[36] W. Balmant, M.H. Sugai-Guérios, J.H. Coradin, N. Krieger, A. Furigo Junior, D.A. Mitchell, A Model for Growth of a Single Fungal Hypha Based on Well-Mixed Tanks in Series: simulation of Nutrient and Vesicle Transport in Aerial Reproductive Hyphae, PLoS ONE 10 (2015) e0120307, doi:10.1371/journal.pone.0120307.
[37] S.S. Schmieder, C.E. Stanley, A. Rzepiela, D. van Swaay, J. Sabotič, S.F. Nørrelykke, A.J. deMello, M. Aebi, M. Künzler, Bidirectional Propagation of Signals and Nutrients in Fungal Networks via Specialized Hyphae, Curr. Biol. 29 (2019) 217–228.e4, doi:10.1016/j.cub.2018.11.058.
[38] polypore | The American Heritage(R) Dictionary of the English Language - Credo Reference, (n.d.). https://search.credoreference.com/content/entry/hmdictenglang/polypore/0 (accessed December 8, 2021).
[39] C. Müller, S. Klemm, C. Fleck, Bracket fungi, natural lightweight construction materials: hierarchical microstructure and compressive behavior of Fomes fomentarius fruit bodies, Appl. Phys. A. 127 (2021) 178, doi:10.1007/s00339-020-04270-2.
[40] C. Wan, Z. Hao, Natural arrangement of micro-strips reduces shear strain in the locust cuticle during power amplification, J. Biomech. 107 (2020) 109842, doi:10.1016/j.jbiomech.2020.109842.
[41] P.-Y. Chen, J. Schirer, A. Simpson, R. Nay, Y.-S. Lin, W. Yang, M.I. Lopez, J. Li, E.A. Olevsky, M.A. Meyers, Predation versus protection: fish teeth and scales evaluated by nanoindentation, J. Mater. Res. 27 (2012) 100–112, doi:10.1557/jmr.2011.332.
[42] F. Barthelat, H. Tang, P.D. Zavattieri, C.-M. Li, H.D. Espinosa, On the mechanics of mother-of-pearl: a key feature in the material hierarchical structure, J. Mech. Phys. Solids. 55 (2007) 306–337, doi:10.1016/j.jmps.2006.07.007.
[43] R. Fogel, Ecological studies of hypogeous fungi. II. Sporocarp phenology in a western Oregon Douglas Fir stand, Can. J. Bot. 54 (1976) 1152–1162, doi:10.1139/b76-124.
[44] M.F. Ashby, R.F.M. Medalist, The mechanical properties of cellular solids, Metall. Trans. A. 14 (1983) 1755–1769, doi:10.1007/BF02645546.
[45] J. Heitman, S.G. Filler, J.E. Edwards, A.P. Mitchell, Molecular Principles of Fungal Pathogenesis, American Society for Microbiology, Washington, DC, 2006.
[46] D. Carlström, The crystal structure of α-chitin (poly-n-acetyl-D-glucosamine), J. Biophys. Biochem. Cytol. 3 (1957) 669–683, doi:10.1083/jcb.3.5.669.
[47] L. Zhao, D. Schaefer, H. Xu, S.J. Modi, W.R. LaCourse, M.R. Marten, Elastic Properties of the Cell Wall of Aspergillus nidulans Studied with Atomic Force Microscopy, Biotechnol. Prog. 21 (2005) 292–299, doi:10.1021/bp0497233.
[48] S.M. Stocks, C.R. Thomas, Strength of mid-logarithmic and stationary phase Saccharopolyspora erythraea hyphae during a batch fermentation in defined nitrate-limited medium, Biotechnol. Bioeng. 73 (2001) 370–378, doi:10.1002/bit.1070.
[49] U.G.K. Wegst, H. Bai, E. Saiz, A.P. Tomsia, R.O. Ritchie, Bioinspired structural materials, Nat. Mater. 14 (2015) 23–36, doi:10.1038/nmat4089.
[50] S. Maurice, G. Arnault, J. Nordén, S.S. Botnen, O. Miettinen, H. Kauserud, Fungal sporocarps house diverse and host-specific communities of fungicolous fungi, ISME J 15 (2021) 1445–1457, doi:10.1038/s41396-020-00862-1.
[51] M.A. Hernández-Oñate, A. Herrera-Estrella, Damage response involves mechanisms conserved across plants, animals and fungi, Curr. Genet. 61 (2015) 359–372, doi:10.1007/s00294-014-0467-5.
[52] M.S. Fischer, N.L. Glass, Communicate and Fuse: how Filamentous Fungi Establish and Maintain an Interconnected Mycelial Network, Front. Microbiol. 10 (2019) 619, doi:10.3389/fmicb.2019.00619.
[53] R. Kahmann, M. Bölker, Self/Nonself Recognition in Fungi: old Mysteries and Simple Solutions, Cell 85 (1996) 145–148, doi:10.1016/S0092-8674(00)81091-0.
[54] D.A. Coomes, K.L. Jenkins, L.E.S. Cole, Scaling of tree vascular transport systems along gradients of nutrient supply and altitude, Biol. Lett. 3 (2007) 86–89, doi:10.1098/rsbl.2006.0551.
[55] K. Baumgartner, M.P.A. Coetzee, D. Hoffmeister, Secrets of the subterranean pathosystem of Armillaria: subterranean pathosystem of Armillaria, Mol. Plant Pathol. 12 (2011) 515–534, doi:10.1111/j.1364-3703.2010.00693.x.